KINK-1, a Novel Small-Molecule Inhibitor of IKKβ, and the Susceptibility of Melanoma Cells to Antitumoral Treatment

Margarete Schön, B. Gregor Wienrich, Susanne Kneitz, Helga Sennefelder, Katharina Amschler, Verena Vöhringer, Olaf Weber, Thorsten Stiewe, Karl Ziegelbauer, Michael P. Schön

Background Increasing the efficacy of chemotherapeutics by reducing chemoresistance may be a useful strategy in cancer therapy. Constitutive activation of nuclear factor-kappa B (NF-κB) is a hallmark of various cancers, including melanoma, which is almost universally resistant to chemotherapy. NF-κB is regulated by inhibitory κB (IκB) proteins, which are in turn phosphorylated by the IκB kinase (IKK) complex.

Methods The effect on NF-κB activity of a novel small-molecule inhibitor of the β subunit of IKK (KINK-1; kinase inhibitor of nuclear factor-κB-1) was assessed by measuring phosphorylation of the α subunit of IκB by immunoblotting, DNA binding by electrophoretic mobility shift assays, and nuclear translocation of NF-κB using immunofluorescence. Regulation of NF-κB–dependent gene expression was determined by microarray analysis, real-time and semiquantitative reverse transcription polymerase chain reaction (RT-PCR), and Western blot analyses. The effects of KINK-1 (alone and in combination with cytostatic agents) on melanoma cells were characterized by assessing proliferation, soft agar colony formation, and markers of apoptosis. The antitumoral efficacy of KINK-1 in combination with the cytostatic agents doxorubicin or camptothecin (all injected intraperitoneally) was tested in vivo by measuring lung weight and counting metastases in C57BL6 mice (groups of six) bearing metastases of melanoma cells. All statistical tests were two-sided.

Results KINK-1 strongly suppressed both constitutive and induced NF-κB activity in melanoma cells. It reduced the expression of NF-κB–dependent gene products that regulate proliferation, cytokine production, and antiapoptotic responses but exhibited little antiproliferative or proapoptotic activity at the cellular level. However, KINK-1 markedly increased the activities of some cytostatic agents in vitro and abrogated doxorubicin-induced NF-κB activation. Combined treatment of C57BL6 mice that had been injected with melanoma cells with KINK-1 and doxorubicin or camptothecin reduced metastases and pulmonary tumor mass compared with either treatment alone (mean lung weight 19 days after injection of melanoma cells of mice treated with 3 mg/kg KINK-1 alone, 1 mg/kg doxorubicin alone, and 1 mg/kg doxorubicin plus 3 mg/kg KINK-1 = 260 mg, 95% confidence interval (CI) = 216 to 305 mg; 268 mg, 95% CI = 224 to 313 mg; and 181 mg, 95% CI = 171 to 192 mg, respectively, $P < .001$ from t tests comparing mean lung weight of double-treated mice to that in mice treated with either compound alone).

Conclusion Inhibition of constitutive and induced IKKβ-activity through treatment with KINK-1 might increase tumor susceptibility to chemotherapy.

J Natl Cancer Inst 2008;100:862–875

Chemoresistance is one of the greatest challenges in cancer management. Melanoma, a highly aggressive tumor arising from pigment cells of the skin, vividly highlights the problem of chemoresistance because it is almost universally resistant to chemotherapy (1–3). The complete response rate to dacarbazine, the only drug thus far approved by the US Food and Drug Administration for treatment of metastatic melanoma, rarely exceeds 5% (4). Numerous other chemotherapeutics and immunologic approaches have also yielded largely sobering results (5–9).

Recent advances in the understanding of the key signaling pathways promoting tumorigenesis have nourished hope that the chemoresistance of tumors can be overcome while limiting unwanted

Affiliations of authors: Rudolf Virchow Center, Deutsche Forschungsgemeinschaft Research Center for Experimental Biomedicine (MS, BGW, HS, KA, TS, MPS), Department of Dermatology (MS, BGW, HS, KA, TS, MPS), and Interdisciplinary Collaborative Clinical Research Center (SK), University of Würzburg, Würzburg, Germany; Department of Dermatology and Venereology, University of Göttingen, Göttingen, Germany (MS, BGW, MPS); BayerHealthCare, Global Drug Discovery, Wuppertal, Germany (VV, OW, KZ).

Correspondence to: Michael P. Schön, MD, Department of Dermatology and Venereology, University Medical Center Göttingen, von-Siebold-Str 3, 37075 Göttingen, Germany (e-mail: michael.schoen@med.uni-goettingen.de).

See "Funding" and "Notes" following "References."

DOI: 10.1093/jnci/djn174

toxic side effects. One important signaling pathway in tumorigenesis is the nuclear factor-kappa B (NF-κB) pathway, whose constitutive activation is a hallmark of various types of hematologic and solid tumors, including melanoma (10–14). All NF-κB family members have a Rel homology domain, which is important for binding to inhibitory κB (IκB) proteins, dimerization, nuclear translocation, and DNA binding (15–17). In cancer cells, NF-κB regulates cell proliferation, controls apoptosis, promotes angiogenesis, and stimulates invasion and metastasis (18,19). Consistent with a role of NF-κB in oncogenesis, inhibition of NF-κB alone or in combination with cancer therapies may lead to tumor cell death or growth inhibition (20–22). Moreover, activation of NF-κB may mediate inducible chemoresistance to anthracycline drugs such as doxorubicin, a cytostatic agent that induces chemoresistance by increasing NF-κB DNA binding activity and transcription of genes related to tumor progression (23).

Phosphorylation of IκB by the IκB kinase complex (IKK; consisting of one α, one β, and two γ subunits) initiates the classical pathway of NF-κB activation. Impairment of IKKβ-mediated activation of NF-κB has a pronounced effect on tumorigenesis in some animal models of inflammation-associated cancer (24–26).

Here we describe KINK-1 (kinase inhibitor of NF-κB-1), the first compound of a novel class of small-molecule substances, which specifically inhibits IKKβ. We investigated the effect of KINK-1 treatment on NF-κB activation and the genes regulated by this transcription factor and characterized its antineoplastic properties (alone and in the presence of chemotherapeutic agents) in vitro, and, using a murine model of metastasis, in vivo.

CONTEXT AND CAVEATS

Prior knowledge

Constitutive activation of nuclear factor-kappa B (NF-κB) occurs in many cancers, and activation of this transcription factor may mediate resistance to chemotherapy.

Study design

The effects of KINK-1, a small molecule that inhibits NF-κB activity, on NF-κB–dependent gene expression, cellular proliferation, and apoptosis of melanoma cells, and on tumor growth in a murine model of pulmonary metastasis were assessed.

Contribution

The study suggested that inhibition of NF-κB markedly increased the efficacy of several currently used cytostatic agents as reflected in effects on gene expression, cell proliferation, apoptosis, and tumor growth in vivo.

Implications

Using agents that specifically prevent NF-κB activation to enhance the susceptibility of tumor cells to cytostatic agents may improve future antitumoral regimens.

Limitations

The study did not address whether the inhibitor would be effective with oral administration, and in vivo data were confined to a single murine model of tumorigenesis that may not be applicable to human cancers.

Methods

Cells and Culture Conditions

Human melanoma cell lines A375, Mel-2a, SK-Mel-23, Mel-HO, MeWo, MV3, LOX, Brown, and MMNH; the murine melanoma cell line B16F10; and the A549, Colo205, DLD-1, HT29, HCT116, U87, HH, EL4, DB, MiaPaCa2, MDA-DB-231, PC3, and HaCaT cell lines derived from various tissues (*see* Table 1) were grown in Dulbecco's Modified Eagle Medium (DMEM) supplemented with 10% fetal calf serum, 100 U/mL penicillin, and 100 μg/mL streptomycin (Gibco, Karlsruhe, Germany). To establish new cultures from lung metastases, tumor nodules were freed from connective tissue and cells were released from small (<1 mm) pieces by trypsin treatment (0.25% at 37°C for 4 hours). The cells were then cultured for 3 days before analysis.

Microarray Hybridization and Data Analysis

Total RNA from A375 melanoma cells treated with vehicle (0.1% DMSO) or KINK-1 (5 μM for 12 or 24 hours) was extracted using the RNeasy Kit according to the manufacturer's instructions (Qiagen, Hilden, Germany). RNA integrity and comparability between samples was tested using a BioAnalyzer (Agilent, Santa Clara, CA). RNA integrity numbers were between 9.4 and 9.7. Reverse transcription, second-strand synthesis, and cleanup of double-stranded cDNA were performed according to the Affymetrix protocols (One-Cycle cDNA Synthesis Kit; Affymetrix, Santa Clara, CA) starting from 2 μg total RNA. Biotin-labeled cRNA was synthesized using the IVT Labelling Kit (Affymetrix). The cRNA concentration and the distribution of cRNA fragment sizes were determined by gel electrophoresis. Fragmented cRNA (15 μg) was used for hybridization of the Human Genome U133 Plus 2.0 GeneChip, and data were analyzed using different R packages from the Bioconductor project (http://www.bioconductor.org/). The resulting signal intensities were normalized by variance stabilization (27). The quality of all datasets was tested by density plot and RNA degradation plot. Genes displaying at least a twofold change in expression with KINK-1 treatment were selected. Two independent analyses were performed for each condition. The average ratio in expression was 1.002 (95% confidence interval [CI] = 0.908 to 1.096), indicating excellent reproducibility of the data.

To evaluate functional categories, we used the Gene Ontology Tree Machine (http://bioinfo.vanderbilt.edu/gotm/), a Web-based platform for interpreting microarray data or other interesting gene sets using Gene Ontology hierarchies. It permits the identification of categories that are enriched in an interesting gene set compared with a reference gene set (eg, genes on the array).

Kinase Assays

Human IKKα and IKKβ were cloned from a Quickclone cDNA library (BD Biosciences Clontech, Palo Alto, CA) by polymerase chain reaction (PCR). The IKKβ kinase assay was performed as previously described (28). IKKα kinase assay conditions were as follows: 0.2 μM (1.5 μg/mL) recombinant IKKα, ATP (0.5 Ci per well [γ-^{33}P]ATP), 0.2 μg/mL full-length glutathione S-transferase–tagged IκBα, 20 mM HEPES (pH 7.6), 20 mM β-glycerophosphate, 1 mM Na_3VO_4, 10 mM $MgCl_2$, 100 mM KCl, 1 mM dithiothreitol (DTT), 0.4 mM phenylmethylsulfonyl fluoride (PMSF) and 0.1 mg/mL bovine serum albumin.

Other enzymes were tested according to published procedures, or results were obtained from MDS pharmacology services (http://www.mdsps.com/).

Measurement of Nuclear Translocation of NF-κB

Cells were cultured in normal medium or in the presence of KINK-1 (5 μM) for 12 hours. Then, cultures were maintained in normal medium or stimulated with tumor necrosis factorα (TNFα) (1 nM for 30 minutes or 2 hours). Cells were rinsed in cold phosphate-buffered saline (PBS), fixed in cold methanol for 10 minutes, and rinsed again in PBS. Cells were then incubated with an anti-p65 antibody (clone F-6, Santa Cruz Biotech, Santa Cruz, CA; 10 μg/mL in PBS) for 45 minutes, washed with PBS, and incubated with a fluorescein isothiocyanate-labeled secondary goat-anti-mouse antibody (DAKO, Hamburg, Germany) for 45 minutes. After a final wash with PBS, the distribution of p65 was examined using a fluorescence microscope.

Cell Lysis and Subcellular Fractionation

To generate whole-cell lysates for Western blotting, 10^7 cultured cells were solubilized in lysis buffer (1% Triton X-100, 50 mM Tris, pH 7.4, 150 mM NaCl, and one tablet of Complete Protease Inhibitor for 10 mL lysis buffer according to the manufacturer's instructions [Boehringer Mannheim, Mannheim, Germany]). To make cytosolic and mitochondrial extracts, 10^7 cells were detached from the culture dishes by scraping into PBS on ice, lysed in hypotonic buffer containing Complete Protease Inhibitor, and incubated on ice for 15 minutes. The cells were then homogenized by repeated passage through a 28-gauge needle and centrifuged at 10 000*g* for 10 minutes at 4°C. Cytosolic fractions were collected from the supernatants, and the mitochondrial pellets were solubilized in lysis buffer (1% Triton X-100 containing Complete Protease Inhibitor).

To generate nuclear extracts, cells were removed from the culture dishes using a cell scraper and centrifuged at 1500*g* for 3 minutes. Pellets were resuspended in buffer A (10 mM HEPES/KOH, pH 7.9; 1.5 mM MgCl2; 10 mM KCl; 0.5 mM DTT; 0.2 mM PMSF) for 3 minutes, centrifuged for 3 minutes at 1000*g*, and resuspended again in 100 μL of buffer A for 30 minutes on ice. Then, 3.2 μL of 10% NP40 was added to the cell suspension, and the cells were centrifuged for 10 minutes at 20 000*g*. The pellet was resuspended in 25 μL of buffer C (20 mM HEPES/KOH, pH 7.9; 25% glycerol; 420 mM NaCl; 1.5 mM $MgCl_2$; 0.2 mM EDTA; 0.5 mM DTT; 0.2 mM PMSF) and incubated for 20 minutes on ice. The resulting nuclear extracts were used for Western blotting.

Western Blot Analysis

For analysis of IκB phosphorylation, melanoma cells (A375, MMNH, and Mel-2a) were either cultured in normal medium, incubated with KINK-1 (5 μM for 12 hours), incubated with KINK-1 (5 μM for 12 hours) followed by TNFα (1 nM for 15 minutes), or incubated with TNFα (1 nM for 15 minutes). Protein concentrations in the cytoplasmic, mitochondrial, and nuclear fractions were determined by Bradford assays. Equal amounts of protein were separated by sodium dodecyl sulfate–polyacrylamide gel electrophoresis and transferred onto nitrocellulose membranes. Proteins of interest were detected by monoclonal antibodies (mAbs) followed by peroxidase-labeled goat-anti-mouse IgG or peroxidase-labeled goat-anti-rabbit IgG and a chemiluminescence reaction (ECL from Amersham Pharmacia, Buckinghamshire, UK). Anti–human Bcl-2 (clone 124, DAKO), anti–human Bax (2D2; Biozol, Eching, Germany), anti–human Bcl-X_L (H-5; Santa Cruz Biotech), and anti–human β-actin (abcam, Biozol) were used at 1 : 1000 dilutions. Anti–human cyclin D1 (DCS6; Cell Signaling, Danvers, MA), anti–human cytochrome c (D-8; BD, Heidelberg, Germany), and anti–human Smac (V-17; Santa Cruz Biotech) were used at a 1 : 100 dilution. Phosphorylated IκB and nonphosphorylated IκB were detected in the cytoplasmic fraction using the B-9 mAb (Santa Cruz, final dilution 1 : 50) or the H-4 mAb (Santa Cruz, final dilution 1 : 50), respectively. Signal intensities were quantitated densitometrically (Fluor-S MultiImager, BioRad, München, Germany).

Electrophoretic Mobility Shift Assays

Melanoma cells cultured in the presence of vehicle (0.1% DMSO) or KINK-1 (5 μM) were incubated with TNFα (1 nM), phorbol 12-myristate 12-acetate (PMA) (25 ng/mL), lipopolysaccharide (LPS) (1 μg/mL), or doxorubicin (1 μM) for 12 hours. Subcellular fractionation and preparation of nuclear extracts was performed as described above (29–31). Nuclear extracts (10 μg) from A375 cells were incubated with the double-stranded NF-κB oligonucleotide 5′-AGTTGAGGGGACTTTCCCAGGC-3′ that had been end-labeled with ^{32}P using the Gel Shift Assay System (Promega, Madison, WI) for 20 minutes at room temperature. Subsequently, the DNA–protein complexes were resolved in a 6.6% native polyacrylamide gel. For supershift assays, nuclear extracts (10 μg) were incubated with antibodies (1 μg) against p65 (F-6), p50 (E-10), or p52 (C-5, all from Santa Cruz Biotech) for 30 minutes at 20°C before analysis by electrophoretic mobility shift assays. Radioactive signals were visualized and quantitated using a PhosphorImager and the Image Quant software (BioRad).

Semiquantitative Reverse Transcription–Polymerase Chain Reaction

RNA from treated or untreated cells was extracted using the RNeasy Mini Kit (Qiagen) according to the manufacturer's instructions. Gene expression was assessed by reverse transcription (RT)-PCR, as previously described (32). The primers and the respective annealing temperatures are indicated in Supplementary Table 1 (available online).

Quantitative Real-Time Polymerase Chain Reaction

cDNA was prepared from RNA of cells treated with vehicle or 5 μM KINK-1 for 4, 12, or 48 hours. PCR was performed according to the manufacturer's instructions using the QuantiTect Primer Assays (Qiagen) for human IL-6, IL-8, IL-1β, CXCL-1, and GAPDH. Each PCR was carried out in triplicate in a 25 μL volume using QuantiTect SYBR Green Kits (Qiagen). Thermal cycles were 5 minutes at 95°C for initial denaturing followed by 40 cycles of 95°C for 10 seconds and 60°C for 30 seconds in the ABI Prism 7000 Sequence Detection System. Values for each gene were normalized to expression of GAPDH. Experiments were done in duplicate.

Proliferation Assays

To determine IC_{50} values for inhibition of cell proliferation, tumor cells were plated at 500 cells per well in RPMI medium

supplemented with glutamax, insulin, transferrin, selenium A, and 10% fetal bovine serum in 96-well plates. After 24 hours, the test compounds (10× final concentration) were added to the cultures and plates were incubated for 72 hours at 37°C in 5% CO_2 in a humidified incubator. Detection of cell growth as evidenced by ATP content with CellTiter-Glo (Promega) was determined according to the manufacturer's instructions. Briefly, CellTiter-Glo reagent was added to the cultures (100 µL per well) and, 10 minutes later, luciferase luminescence was measured using a luminescence charge-coupled device camera system.

To assess the combined effects of KINK-1 and other compounds, cells were plated at a density of 3000 cells per well in a 96-well plate. Subconfluent cultures were treated with KINK-1 (5 µM), doxorubicin (0.3 µM or 1.0 µM), camptothecin (10 µM or 30 µM), tamoxifen (10 µM or 30 µM), cisplatin (10 µM or 30 µM), or combinations of the cytostatic agents with KINK-1, in a final volume of 100 µL. After 24 or 48 hours, cell proliferation was measured using the CellTiter 96 AQueous One Solution Cell Proliferation Assay (Promega), a form of the 3-(4,5-dimethylthiazol-2-yl)-5-(3-carboxymethoxyphenyl)-2-(4-sulfophenyl)-2H-tetrazolium (MTS) assay.

Detection of Mitotic Cells In Vivo

Paraffin-embedded sections of mouse lungs were rehydrated, washed twice with Sörensen buffer (15 mM $Na_2HPO_4 \times 2H_2O$ and 15 mM $KH_2PO_4 \times H_2O$, pH 6.8), incubated for 3 minutes with PBS containing 62.5 µg/mL acridine orange, and destained for 8 minutes in Sörensen buffer (33). Mitotic cells were immediately visualized by fluorescence microscopy. The proliferation index (PI, number of proliferating cells per 100 tumor cells) was determined in a blinded fashion by counting at least 2000 cells per section in at least four independent tissues for each condition.

Induction and Detection of Apoptosis (DNA Fragmentation Assay)

To assess apoptotic responses, cultured cells were incubated with apoptotic stimuli for 16 hours. The following cytostatic agents were used to trigger apoptosis: doxorubicin (0.3 or 1.0 µM), camptothecin (10 µM or 30 µM), and tamoxifen (10 µM or 30 µM). To trigger CD95 (Fas)–mediated apoptosis, the cells were incubated with the Fas-stimulating CH-11 mAb (1 µg/mL). To stimulate the TRAIL (TNF-related apoptosis-inducing ligand) receptor system, 10 ng/mL of the natural ligand (TRAIL, R&D Systems, Wiesbaden, Germany) was added to the cultures. To inhibit caspase activity, cells treated with 5 µM KINK-1, 1 µM doxorubicin, or their combination were cultured in the absence or presence of the general caspase inhibitor zVAD-FMK (R&D Systems) at a final concentration of 10 nM. Cells were preincubated with zVAD-FMK for 10 minutes before incubation with the apoptotic stimulus for 24 hours. Control cultures were treated with 0.1% DMSO.

After the treatments, the cells were lysed and centrifuged at 10000 × *g* for 10 minutes to prepare a clear supernatant. Equal amounts of the supernatant were added to microtiter plates coated with anti-histone antibodies (clone H11-4) and incubated for 90 minutes at 20°C. Histone-bound DNA fragments were detected using the Cell Death Detection ELISA (Roche Diagnostics, Penzberg, Germany). The substrate reaction (for determination of the amount of peroxidase retained in the immunocomplex with ABTS (2,2′-azino-di-[3-ethylbenzthiazoline sulfonate (6)] as a substrate) was quantified using an ELISA reader at a wavelength of 405 nm.

Double Thymidine Treatment for G1/S Synchronization and Cell Cycle Analysis

Subconfluent A375 cell cultures were incubated with 2 mM thymidine for 16 hours, washed three times with PBS, and grown in DMEM containing 0.5% fetal calf serum (FCS) for 10 hours. Then, 2 mM thymidine was added and cells were incubated for another 14 hours. Cells were washed again three times with PBS and then released with 10% FCS-containing medium for 4, 12, and 24 hours. Thymidine-treated cells and nonsynchronized A375 cells were treated with DMSO (control), 26 nM bortezomib, or up to 25 µM KINK-1. For cell cycle analysis, the fixed cells (70% ethanol on ice) were washed three times and resuspended in cold PBS containing 5 µg/mL propidium iodide and 0.1 mg/mL RNase A. Flow cytometry was performed using the FACS Calibur and Cell Quest software.

Experimental Pulmonary Metastasis

Mouse experiments were approved by the appropriate authorities (Regierung von Unterfranken, Würzburg, Germany). Mice were housed in a climate-controlled specific pathogen–free (SPF) facility, and, at the time of termination of the experiments, were killed by ether anesthesia followed by cervical dislocation according to institutional guidelines. In the first series of experiments, therapeutic effects on the early phases of metastasis were evaluated. C57BL6 mice (n = 6 mice per group) were injected into the tail vein with 2.5×10^5 B16F10 murine melanoma cells. Treatment (by intraperitoneal injection) was started 1 day after injection of the melanoma cells. Treatment regimens were as follows: group 1, vehicle (10% cremophor in H_2O); group 2, 10 mg/kg KINK-1 every other day; group 3, 3 mg/kg KINK-1 every other day; group 4, 4 mg/kg doxorubicin twice weekly; group 5, 1 mg/kg doxorubicin twice weekly; group 6, 10 mg/kg KINK-1 every other day and 4 mg/kg doxorubicin twice weekly; group 7, 3 mg/kg KINK-1 every other day and 1 mg/kg doxorubicin twice weekly. Number of metastases and mean lung weight, a surrogate for pulmonary tumor mass, were evaluated 19 days after injection of the melanoma cells.

To assess therapeutic effects in already established metastases, C57BL6 mice (n = 6 mice per group) were injected intravenously with 2.5×10^5 B16F10 cells, and treatment was started 8 days after transplantation. The mice received an initial high-dose bolus (group 1, vehicle; group 2, 10 mg/kg KINK-1; group 3, 4 mg/kg doxorubicin; group 4, 10 mg/kg KINK-1 and 4 mg/kg doxorubicin. Lower doses were administered on days 2, 5, 7, and 9: group 1, vehicle; group 2, 3 mg/kg KINK-1; group 3, 1 mg/kg doxorubicin; group 4, 3 mg/kg KINK-1 and 1 mg/kg doxorubicin). Metastasis was evaluated 12 days after initiation of treatment (for ethical reasons, mice had to be euthanized at this time point and could not be observed for longer periods of time).

Statistical Analyses

Data were calculated as the mean values with 95% confidence intervals. Statistical comparisons were performed using Excel software (Microsoft GmbH, Munich, Germany). Results were

compared using the Student *t* test, and *P* values less than .05 (95% CI) were considered statistically significant. All statistical tests were two-sided.

Results

KINK-1 and Selective Inhibition of IKKβ Activity

To identify small-molecule compounds that interfere with the activation of NF-κB in tumor cells, small-molecule IKKβ inhibitors were derived from a large-scale high-throughput screening (28). In a series of cell-free experiments, compound A (7-[2-(cyclopropylmethoxy)-6-hydroxyphenyl]-5-[(3S)-3-piperidinyl]-1,4-dihydro-2H-pyrido [2,3-d][1,3] oxazin-2-one hydrochloride), with M_r 395.45 (Figure 1, A), specifically inhibited the kinase activity of human recombinant IKKβ with a K_i of 2 nM for ATP and 4 nM for the GST-IκBα substrate. The selectivity of the compound was confirmed by assessing its effects on additional enzymes including various kinases (IKKα, IKK3, Syk, ERK-1, PI3Kg, Fyn, Lck, PKA, PKC, MKK4, and MKK7), phosphatases (PTP1B, PTP1C, PTP [T cell], CD45, and PP2B), phospholipases (PLC and PLA2-I), and proteases (caspase-1,-3,-4,-6,-7, and -8 and matrix metalloprotease-1,-2,-3,-7, and-9) in cell-free assays (data not shown). Compound A

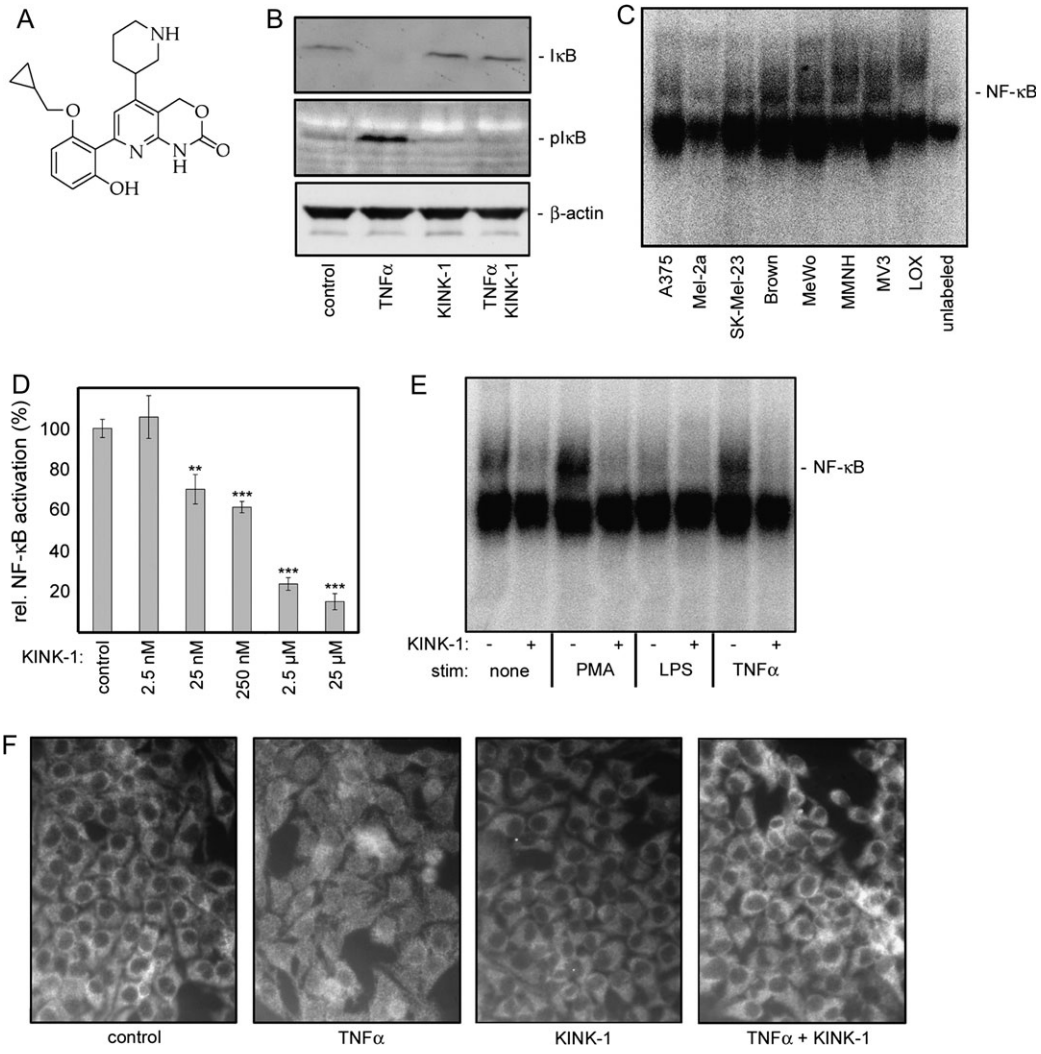

Figure 1. Inhibition of IκB phosphorylation, NF-κB activation, and nuclear translocation by KINK-1. **A**) Chemical structure of KINK-1. **B**) Western blot showing total IκB (upper panel), phosphorylated IκB (middle panel), and the housekeeping protein β-actin (lower panel) in lysates of A375 melanoma cell cultures treated with normal medium (control), tumor necrosis factorα (TNFα; 1 nM), KINK-1 (5 μM), or both. **C**) Activation of NF-κB in various melanoma lines. Cells were lysed, nuclear extracts were prepared, and activated NF-κB was determined by electrophoretic mobility shift assays (EMSA). Unlabeled refers to an A375 extract incubated with a 10-fold excess of unlabeled oligonucleotides to demonstrate the specificity of the upper band. **D**) Percent activation of NF-κB in nuclear extracts of A375 melanoma cells cultured in normal medium (control) or in the presence of the indicated concentrations of KINK-1 (corresponding to the fraction of the labeled probe bound) was quantitated densitometrically. Values shown are the mean of triplicate measurements. $^{**}P = .007$; $^{***}P < .001$ compared with untreated control. **E**) Activated NF-κB in nuclear extracts from A375 melanoma cells cultured in normal medium (lanes 1 and 2), in the presence of phorbol 12-myristate 12-acetate (PMA) (25 ng/mL; lanes 3 and 4), lipopolysaccharide (LPS) (1 μg/mL; lanes 5 and 6), or TNFα (1 nM; lanes 7 and 8), and supplemented with vehicle (0.1% DMSO) or KINK-1 (5 μM). The fraction of activated NF-κB was determined by EMSA. **F**) Analysis of nuclear translocation of NF-κB in A375 melanoma cells cultured in normal medium (panels 1 and 2) or in the presence of KINK-1 (5 μM; panels 3 and 4) and maintained in normal medium (panels 1 and 3) or stimulated with TNFα (1 nM; panels 2 and 4) was determined by immunofluorescence. The photomicrographs were taken 30 minutes after stimulation with TNFα; similar results were obtained when the cells were stimulated with TNFα for 2 hours.

had no detectable inhibitory activity toward these enzymes, with the exception of the IKKβ-related kinase IKKα, for which the K_i (135 nM) was approximately 70-fold higher than for IKKβ. Thus, the compound is a highly selective IKKβ inhibitor. We termed this member of a novel class of IKK inhibitors KINK-1.

KINK-1 and Inhibition of IκB Phosphorylation in Melanoma Cells

As part of the IKK complex, the primary function of IKKβ is activation of NF-κB via phosphorylation of IκB (34). By probing Western blots with an antibody specific for the phosphorylated form of IκB, we found that the protein was constitutively phosphorylated in human melanoma cells (data not shown). When three melanoma lines (A375, MMNH, and Mel-2a) that showed constitutive phosphorylation of IκB were incubated with 5 μM KINK-1, viability, proliferation, and apoptosis were not affected (data not shown). However, both constitutive and TNF-induced phosphorylation of IκB was inhibited by KINK-1 (Figure 1, B, representative of all cell lines tested).

KINK-1 and Reduced NF-κB Activation in Melanoma Cells

Following dissociation of the IκB/NF-κB complex, activated NF-κB translocates from the cytoplasm into the nucleus, where it binds to specific DNA sequences and thereby regulates transcription of various genes (15,16). Because electrophoretic mobility shift assays are a reliable method for detecting DNA-binding proteins, we used them to detect activated NF-κB in the nuclear fractions of cell lysates. In nuclear fractions from melanoma cells, we observed constitutive activation of NF-κB (Figure 1, C), and KINK-1 substantially decreased NF-κB activation in a dose-dependent manner (Figure 1, D and E; the presence of the p65 subunit within the upper band was confirmed by supershift assays; Supplementary Figure 1, available online). Furthermore, when activation of NF-κB was induced with TNFα (1 nM) or PMA (25 ng/mL) [which activate NF-κB through different pathways upstream of the IKK complex (35)], KINK-1 treatment (5 μM) led to almost complete abrogation of NF-κB activation (Figure 1, E). Similar results obtained with the keratinocyte-derived line HaCaT (data not shown) suggested that the inhibitory activity of KINK-1 is not specific to particular cell types (data not shown).

Because translocation of activated NF-κB from the cytoplasm to the nucleus is necessary for its proper function, we visualized nuclear translocation of NF-κB in three melanoma cell lines (A375, MMNH, and Mel-2a), using an immunofluorescence method to detect p65. Incubation of melanoma cells with TNFα (1 nM for 30 minutes) resulted in rapid nuclear translocation of NF-κB, whereas pretreatment of the cells for 12 hours with KINK-1 (5 μM) abolished this effect (Figure 1, F). Thus, KINK-1 suppressed both constitutive and induced phosphorylation of IκB, as well as downstream activation of NF-κB.

KINK-1 and Differential Reduction of Expression of NF-κB–Dependent Gene Products

NF-κB is an important transcription factor that regulates transcription of a multitude of genes, many of which have a role in cell proliferation, migration, or adhesion. To further investigate the downstream effect of KINK-1–mediated inhibition of IKKβ, we used microarray analyses to assess the expression of approximately 54000 genes in A375 melanoma cells that were exposed to KINK-1 for 12 or 24 hours. We found that for 124 genes, there was at least a twofold alteration in expression compared with untreated cells; for 16 of these genes, there was a more than fourfold difference between melanoma cells treated with KINK-1 and untreated cells (a subset of these genes classified in terms of function is shown in Figure 2, A). To confirm the KINK-1-mediated reduction in expression of NF-κB–dependent gene products, we measured the transcription of 14 genes by RT-PCR. We selected several gene products known to be regulated by NF-κB as well as some gene products regulated independent of NF-κB to further demonstrate the specificity of KINK-1. Gene products whose transcription was diminished by KINK-1 included CCL-2 (MCP-1), CXCL-1 (Gro-α), CXCL-8 (IL-8), TNFα, IL-6, MMP-9, COX-2, and ICAM-1-1 (Figure 2, B). Similar effects of KINK-1 treatment on expression of these genes were observed in cells treated with the potent activators of NF-κB, TNFα (1 nM), or PMA (25 ng/mL) (Figure 2, B). Time-dependent reductions in the expression of IL-1β, IL-6, CXCL-1, and CXCL-8 were confirmed by quantitative real-time PCR (data not shown). Expression of other gene products, such as β-catenin, p21, and VEGF, were affected marginally, if at all, by KINK-1. The results of the semiquantitative RT-PCR and the quantitative real-time PCR regarding expression of IL-6 and CXCL-8 (gene products that were assessed by both techniques) were in good agreement (Figure 2, C and D).

Because cellular apoptosis and cell cycle regulation are often dysregulated in malignant tumors and because some apoptosis-related and cell cycle–related gene products such as IAP (inhibitors of apoptosis) proteins, members of the Bcl-2 family, or cyclins may be influenced by NF-κB, we assessed components of the apoptotic signaling cascade in melanoma cells treated with KINK-1. KINK-1 treatment induced moderate release of mitochondrial Smac and cytochrome c into the cytoplasm (Figure 2, C), where it contributes to the formation of the apoptosome, and decreased the expression of the antiapoptotic proteins Bcl-X_L and cyclin D1 (data not shown). In contrast, the Bcl-2/Bax ratio was only marginally affected (Figure 2, C). In addition, in melanoma cells treated simultaneously with doxorubicin and KINK-1, there was a marked decrease in expression of gene products related to tumor progression as determined by RT-PCR (Figure 2, D). These gene products included cytokines and chemokines involved in tumor cell migration and angiogenesis (CCL-2 [MCP-1], CXCL-8 [IL-8] and IL-6), a matrix-degrading enzyme that promotes tumor invasion (the matrix metalloprotease MMP-9), and the adhesion molecule ICAM-1, which mediates tumor cell adhesion.

Overall, there was a clear tendency toward reduced expression of genes involved in cell proliferation, motility, and protection against apoptotic signals in KINK-1–treated melanoma cells (Figure 2). The activity of KINK-1 in melanoma cells was similar regardless of whether activation of NF-κB was constitutive or subsequent to treatment with TNF, LPS, PMA, or doxorubicin (Figure 2, B and D).

KINK-1 and Direct Toxicity

Because KINK-1 affected the expression of several gene products thought to mediate important cellular functions, including

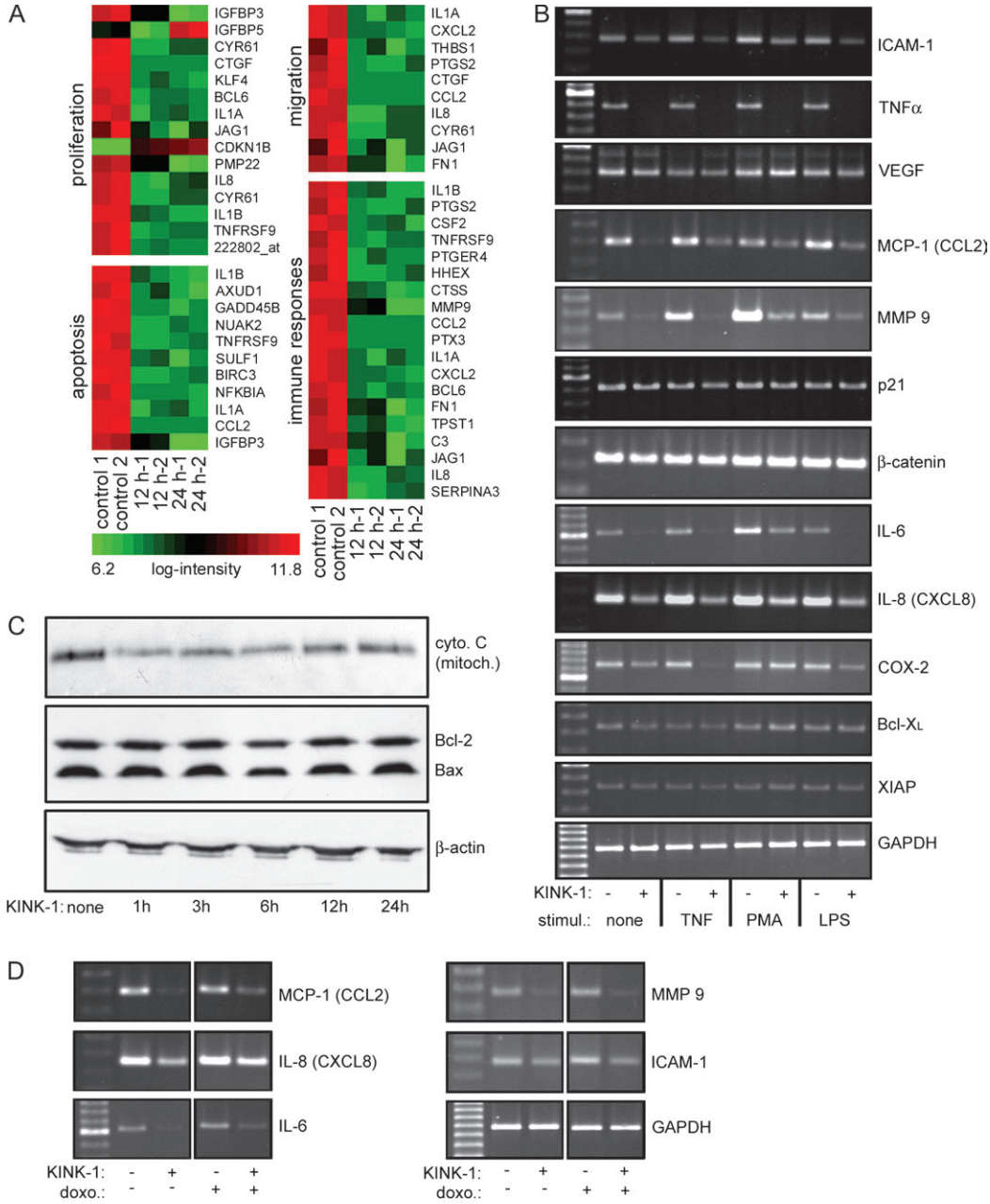

Figure 2. Differential inhibition of the expression of NF-κB–dependent gene products by KINK-1. **A**) Microarray cluster analysis (**heat plots**) of A375 melanoma cells cultured in normal medium (left) or in the presence of KINK-1 (5 μM) for 12 (middle) or 24 (right) hours. The panels show gene products with more than twofold changes compared with the control culture from two independent experiments (labeled 1 and 2, respectively). The panel depicts a selection of genes from different functional panels. **Red** color indicates higher and **green** color indicates lower expression. **B**) Differential regulation of NF-κB–dependent genes by KINK-1 in melanoma cells under both resting and stimulated conditions detected by semiquantitative reverse transcription-polymerase chain reaction (RT-PCR). A375 melanoma cells were cultured in normal medium (lanes 1 and 2) or stimulated with TNFα (1 nM; lanes 3 and 4), phorbol 12-myristate 12-acetate (PMA) (25 ng/mL; lanes 5 and 6), or lipopolysaccharide (LPS) (1 μg/mL; lanes 7 and 8) for 12 hours and maintained in medium containing vehicle or KINK-1 (5 μM) as indicated at the bottom of the panels. **C**) Western blot of cytochrome c from mitochondrial extracts and Bcl-2/Bax from whole-cell lysates of MMNH melanoma cells exposed to KINK-1 (5 μM) for the indicated periods of time. **D**) RT-PCR analysis of gene expression in A375 melanoma cells cultured in normal medium (lanes 1 and 2) or in the presence of doxorubicin (1 μM; lanes 3 and 4) and maintained in medium containing vehicle or KINK-1 (5 μM) as indicated at the bottom of the panels.

proliferation and apoptosis, we determined whether KINK-1 causes toxicity at the cellular level by assessing proliferation and apoptosis of tumor cells. The results of proliferation assays with 14 tumor cell lines confirmed that at nanomolar concentrations the cytostatic agents taxol and camptothecin statistically significantly inhibited proliferation (data not shown). In contrast, the IC_{50} of KINK-1 in assays of cellular proliferation was approximately 1000-fold higher than that of any of these agents for inhibition of growth of 14 different tumor cell lines (Table 1). The low cytotoxicity of KINK-1 was confirmed by assaying the colony formation of six different

tumor lines (data not shown). Human melanoma cells A375 and murine B16F10 cells exposed to 5 μM KINK-1 showed no change in cellular morphology (Figure 3, A). In cultured melanoma cell lines, statistically significant antiproliferative and proapoptotic effects were observed only at concentrations of 10 μM and higher, as determined by DNA fragmentation assays (data not shown) and MTS proliferation assays: proliferation of untreated A375 cells = 2.175 U, 5% CI = 1.870 to 2.480 U; proliferation of cells treated with 10 μM KINK-1 = 1.525 U, 5% CI = 1.198 to 1.852 U, $P = .048$ in comparison to untreated cells; and proliferation of cells treated with 15 μM KINK-1 = 0.725 U, 95% CI = 0.537 to 0.913 U, $P < .001$. This low toxicity at the cellular level was observed despite the fact that inhibition of NF-κB was detectable at markedly lower concentrations.

The suppressive effect of KINK-1 on cyclin D1 expression suggested that KINK-1 might inhibit cell cycle regulation in melanoma cells. To test this hypothesis, melanoma cells (A375, Mel-2a, and MMNH) were exposed to higher doses of KINK-1 (≥10 μM) for extended periods of time (ie, 4, 12, and 24 hours). As determined by flow cytometry of propidium iodide–labeled cells, cell cycle was arrested in the G2 phase. However, whereas the proteasome inhibitor bortezomib led to permanent cell cycle arrest under these conditions, KINK-1–treated cells appeared to re-enter the cell cycle (Supplementary Figure 2, available online).

Thus, KINK-1 exhibited very low antiproliferative and pro-apoptotic effects at the cellular level, and the concentrations of KINK-1 required to produce toxic effects in vitro were several logs higher than those for established cytostatics. Therefore, KINK-1 may have low or negligible cytotoxic potential at concentrations sufficient to inhibit NF-κB.

Table 1. Antiproliferative activity of KINK-1 in cancer cell lines*

Cell line	IC_{50} (μM)	95% CI	Number of experiments
B16F10 (murine melanoma)	14	12 to 16	9
MeWo (human melanoma)	19	11 to 26	3
Colo205 (human colon carcinoma)	20	15 to 25	6
DLD-1 (human colon carcinoma)	21	20 to 22	3
HT29 (human colon carcinoma)	18	14 to 22	4
HCT116 (human colon carcinoma)	21	16 to 26	3
U87 (human glioblastoma)	9.9	9.6 to 10	2
HH (human lymphoma)	2.8	2.2 to 3.4	6
EL4 (murine lymphoma)	12	6.3 to 18	5
DB (human lymphoma)	12	11 to 13	3
MiaPaCa2 (human pancreas carcinoma)	19	14 to 23	5
MDA-MB-231 (human breast carcinoma)	18	11 to 25	2
PC3 (human prostate carcinoma)	18	12 to 24	3
A549 (human lung carcinoma)	17	15 to 19	6

* IC_{50} values (ie, compound concentration that inhibits proliferation by 50%) were calculated from several independent experiments for each condition. KINK-1 = kinase inhibitor of nuclear factor-κB-1; CI = confidence interval.

KINK-1 and Increased Susceptibility of Melanoma Cells to Antitumoral Treatment

The strong inhibitory effect of KINK-1 on the expression of gene products involved in cell cycle regulation, proliferation, or apoptosis resistance, together with its surprisingly low cytotoxic and proapoptotic activity at the cellular level, led us to hypothesize that inhibition of IKKβ by KINK-1 would increase the susceptibility of tumor cells to antitumoral treatment and/or antagonize mechanisms of chemoresistance. To test this hypothesis, we treated three melanoma cell lines (A375, MMNH, and B16F10) with several well-characterized cytostatic compounds, different concentrations of TRAIL, or the CD95 (Fas)–agonistic proapoptotic CH-11 mAb in either the presence or absence of KINK-1. Cell proliferation was assessed by MTS assays, and apoptosis was determined by DNA fragmentation. KINK-1 at concentrations as high as 7.5 μM did not induce apoptosis in any of the melanoma cell lines. Doxorubicin alone did not induce apoptosis at concentrations of 0.1 μM or 0.3 μM and showed only weak proapoptotic activity at 1.0 μM. However, the inhibition of cell proliferation by doxorubicin as determined by the MTS assay was statistically significantly enhanced when KINK-1 was present in the cell cultures: proliferation (arbitrary units) of untreated A375 cells = 2.24 U, 95% CI = 2.12 to 2.36 U; proliferation of cells treated with 5 μM KINK-1 = 2.18 U, 95% CI = 1.93 to 2.42 U; proliferation of cells treated with 0.3 μM doxorubicin = 2.01 U, 95% CI = 1.86 to 2.16 U; and proliferation of cells treated with 0.3 μM doxorubicin and 5 μM KINK-1 = 1.12, 95% CI = 0.97 to 1.27, $P < .001$, compared with doxorubicin (0.3 μM) alone; proliferation of cells treated with 1.0 μM doxorubicin = 1.52 U, 95% CI = 1.40 to 1.64 U; proliferation of cells treated with 1.0 μM doxorubicin and 5 μM KINK-1 = 0.54 U, 95% CI = 0.40 to 0.68 U, $P < .001$, compared with doxorubicin (1.0 μM alone; Figure 3, C). The antiproliferative activities of tamoxifen and camptothecin, but not cisplatin, were similarly increased by KINK-1 (Figure 3, C). Furthermore, apoptosis (as measured by the generation of histone-bound DNA fragments) of melanoma cells was increased by the presence of KINK-1 at low concentrations of doxorubicin: with treatment with 0.3 μM doxorubicin, the increase in apoptosis in the presence of 3 μM KINK-1 = 1.8-fold, 95% CI = 1.63- to 1.95-fold, $P = .002$, and the increase in the presence of 5 μM KINK-1 = 2.4-fold, 95% CI = 2.21- to 2.55-fold, $P < .001$; with treatment with 1.0 μM doxorubicin, the increase with 3 μM KINK-1 = 2.5-fold, 95% CI = 2.18- to 2.84-fold, $P = .005$, and the increase with treatment with 5 μM KINK-1 = 3.5-fold, 95% CI = 3.15- to 3.83-fold, $P < .001$ (Figure 3, D). A similar enhancement of proapoptotic activity was observed when the cytostatic agents camptothecin or tamoxifen were combined with KINK-1 (Figure 3, D). Likewise, the apoptotic response was increased when the natural death receptor ligand TRAIL or the CD95-activating CH-11 mAb was combined with KINK-1 (data not shown). Thus, specific inhibition of IKKβ by KINK-1 markedly increased the susceptibility of melanoma cells to some antitumoral treatments in vitro.

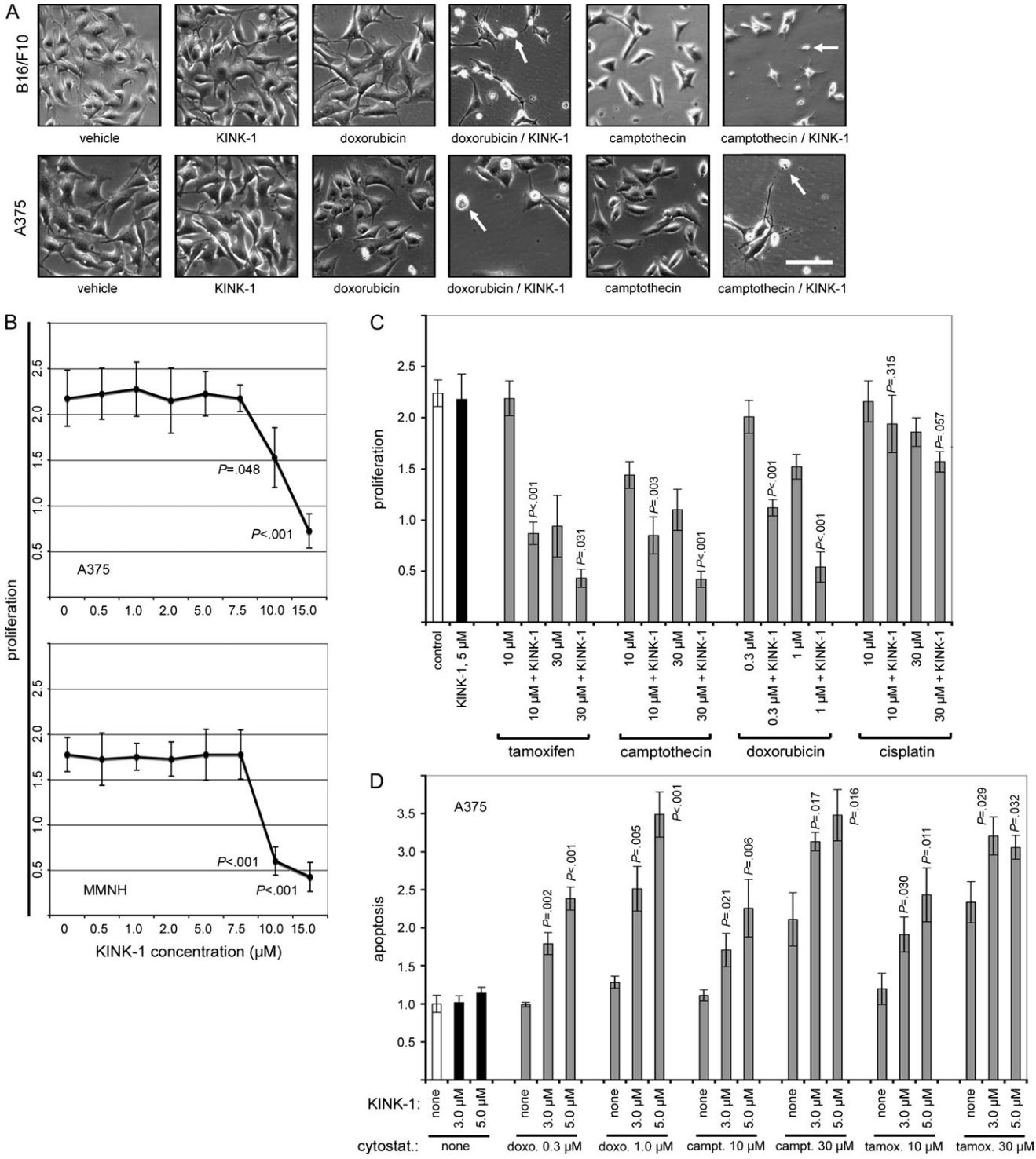

Figure 3. Toxicity of KINK-1 and its effect on susceptibility of melanoma cells to antitumoral treatment in vitro. **A**) Murine (B16F10) and human (A375) melanoma cells were cultured for 24 hours in the presence of doxorubicin (1.0 μM), camptothecin (10.0 μM), or KINK-1 (5 μM). KINK-1 alone had no apparent effect on cellular morphology, whereas combinations of doxorubicin or camptothecin and KINK-1 resulted in marked cellular damage (**arrows** indicate examples of damaged cells). Scale bar = 20 μm. **B**) Proliferation (fold increase in number of cells as reflected by the MTS assay) of two melanoma cell lines (A375 and MMNH) exposed to the indicated concentrations of KINK-1 for 24 hours. Values shown represent the means (**error bars** indicate 95% confidence intervals [CI]) of four cell cultures. **C**) Proliferation in melanoma cells (A375) incubated with normal medium (**open bar**) or the indicated concentrations of tamoxifen, camptothecin, doxorubicin, or cisplatin for 24 hours in the presence or absence of KINK-1 (5.0 μM). Mean values and 95% CIs derive from measurements of four cell cultures. *P* values represent statistical comparisons (two-sided *t* test) of the indicated values vs those obtained when treatment was with the cytostatic alone. **D**) Apoptosis of melanoma cells (A375) incubated with normal medium or the indicated concentrations of doxorubicin (doxo.), camptothecin (campt.), or tamoxifen (tamox.) for 24 hours in the presence or absence of KINK-1 (3.0 μM or 5.0 μM). Y axis indicates the number of apoptotic cells for a given treatment normalized to the number of apoptotic cells without treatment. *P* values represent statistical comparisons (two-sided *t* test) of the indicated values vs treatment with the respective cytostatic agent alone.

KINK-1 and Antagonization of Doxorubicin-Induced Activation of NF-κB

Because drug-induced activation of NF-κB is an important mechanism for resistance to some cytostatics such as doxorubicin (23,36), we tested the hypothesis that IKKβ inhibition by KINK-1 prevents this activation. Doxorubicin treatment led to the activation of NF-κB in all melanoma lines tested. However, when doxorubicin was combined with 5 μM KINK-1, induction of NF-κB activation in a human (A375) and a murine (B16F10) melanoma line was prevented (Supplementary Figure 3, available online).

KINK-1 and Increased Antitumoral Activity of Doxorubicin In Vivo

The inhibition of IKKβ in tumor cells by KINK-1 in vitro featured three interesting properties: 1) KINK-1 showed low direct toxicity, 2) it enhanced the antitumoral activity of cytostatic compounds, and 3) it antagonized doxorubicin-induced activation of NF-κB, a potential mechanism for resistance to doxorubicin. Based on these results, we performed experiments to investigate the antitumoral activity of KINK-1 in mice.

We examined C57BL6 mice that were injected intravenously with B16F10 melanoma cells and observed that prominent pulmonary metastasis occurred within 19 days in vehicle-treated animals as well as in mice treated with KINK-1 (3.0 mg/kg or 10.0 mg/kg every other day) or doxorubicin (1.0 mg/kg twice weekly) (Figure 4, A–C). Monotherapy of animals injected with tumor cells with higher doses of doxorubicin (4 mg/kg) was severely toxic and led to cachexia. However, after combined treatment with both compounds at doses that were ineffective when given separately, there was a clear and statistically significant reduction in the number of pulmonary metastases and the overall lung weight (a surrogate parameter for pulmonary tumor mass): mean lung weight of vehicle-treated control mice = 248 mg, 95% CI = 230 to 265 mg; mean lung weight of mice treated with 3 mg/kg KINK-1 = 260 mg, 95% CI = 216 to 304 mg; mean lung weight of mice treated with 10 mg/kg KINK-1 = 249 mg, 95% CI = 227 to 271 mg; mean lung weight of mice treated with 1 mg/kg doxorubicin = 268 mg, 95% CI = 224 to 313 mg; mean lung weight of mice treated with 4 mg/kg doxorubicin = 157 mg, 95% CI = 144 to 169 mg; mean lung weight of mice treated with 10 mg/kg KINK-1 plus 4 mg/kg doxorubicin = 133 mg, 95% CI = 128 to 139 mg; mean lung weight of mice treated with 3 mg/kg KINK-1 plus 1 mg/kg doxorubicin = 181 mg, 95% CI = 171 to 192 mg, $P < .001$ from t test comparing mean lung weight of mice treated with the combination of 3 mg/kg KINK-1 plus 1 mg/kg doxorubicin to that in mice treated with 1 mg/kg doxorubicin alone, 3 mg/kg KINK-1 alone, or vehicle-treated controls (Figure 4, B). The increased antitumoral efficacy of combined treatment was confirmed by histological and morphometric analyses of the lungs, which revealed a statistically significant reduction in the areas covered by tumor masses in mice treated with combination treatment compared with mice treated with either treatment alone or with vehicle (Figure 4, C; P values from Student t test comparing combination treatment with either treatment alone or vehicle < .001).

When mitotic cells within pulmonary metastases of the above experiments were visualized by acridine orange staining, a high PI was calculated for vehicle-treated mice and mice treated with KINK-1 or doxorubicin monotherapy (PI in vehicle-treated mice = 1.64, 95% CI = 1.40 to 1.87; PI in KINK-1-treated mice = 1.63, 95% CI = 1.38 to 1.88; PI in doxorubicin-treated mice = 0.86, 95% CI = 0.62 to 1.10; Figure 4, D). By contrast, when low doses of doxorubicin were combined with KINK-1, there was a statistically significant reduction of the PI (PI = 0.22, 95% CI = 0.09 to 0.35; P values < .001 from t tests comparing PI of cells treated with both agents to that of cells treated with KINK-1 or doxorubicin alone, Figure 4, D).

In another series of experiments, mice were injected with B16F10 melanoma cells and left untreated for 8 days to allow tumor growth. Mice were then treated for another 12 days with vehicle, doxorubicin, or a combination of doxorubicin with KINK-1. Again, when mice were treated with a combination of doxorubicin and KINK-1, the lung weights were statistically significantly lower compared with those of either vehicle or doxorubicin-treated mice ($P < .001$ in both cases; Figure 4, E).

To confirm that KINK-1 enhanced the effects of other cytostatic agents, C57BL6 mice injected with B16F10 melanoma cells were treated with camptothecin (2 mg/kg every other day), KINK-1 (3 mg/kg every other day), or both agents. After 19 days, mice treated with KINK-1 or camptothecin alone had developed numerous pulmonary metastases (mean = 113.5, 95% CI = 71.2 to 155.8, and 60.3, 95% CI = 28.3 to 84.9, respectively). Treatment with both KINK-1 and camptothecin led to a statistically significant reduction in the number of pulmonary metastases (mean = 2.0, 95% CI = 1.2 to 2.8; $P = .002$ from t test comparing number of metastases with those observed in mice treated with KINK-1 alone, $P = .01$ comparing number of metastases with those observed in mice treated with camptothecin alone).

Because induction of chemoresistance is a major challenge in many antitumoral therapies and previous studies have demonstrated that doxorubicin may rapidly induce chemoresistance (37), we tested the hypothesis that KINK-1, alone or in combination with doxorubicin, induces chemoresistance in melanoma cells in vivo. Cultures from pulmonary metastases of mice treated with vehicle, KINK-1 (3.0 mg/kg or 10.0 mg/kg), doxorubicin (1.0 mg/kg or 4.0 mg/kg), or combinations thereof were established after 19 days of therapy. Three separate cultures were established for each treatment condition, and the responses of the recultured melanoma cells to KINK-1, doxorubicin, or their combinations were assessed by analyzing proliferation and apoptosis. All of the melanoma cell populations showed almost identical responses: exposure to KINK-1 (5 μM) or doxorubicin (0.3 μM) alone neither inhibited cell proliferation nor statistically significantly induced apoptosis, but the combination of suboptimal concentrations of the two compounds resulted in statistically significant antiproliferative and proapoptotic activity (data not shown). Thus, the response of tumor cells reestablished from treated mice was not distinguishable from the response of the parental cell line.

Discussion

NF-κB signaling pathways are constitutively active in many cancer cells and have been implicated in tumor progression and tumor resistance to chemotherapy (38). Some chemotherapeutic agents may induce chemoresistance of cancer cells through activation of

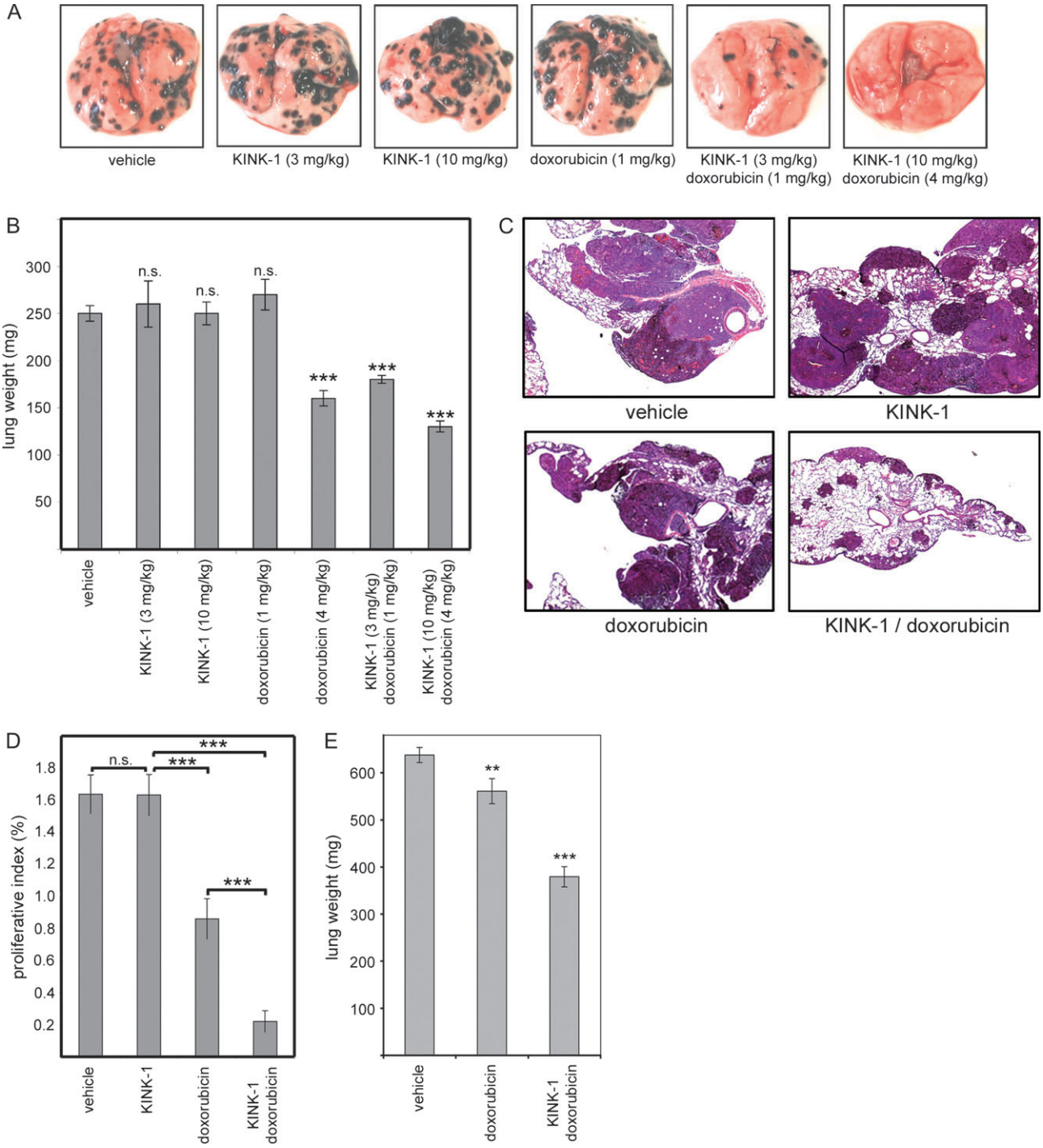

Figure 4. Response of melanoma cells to antitumoral treatment in vivo. **A**) Pulmonary metastasis in C57BL6 mice intravenously injected with 2×10^5 B16F10 melanoma cells and treated with KINK-1 intraperitoneally every other day and/or doxorubicin twice weekly at the indicated doses. **B**) C57BL6 mice (n = 6 per group) were injected intravenously with 2×10^5 B16BL6 melanoma cells and treated as indicated. Total lung weight, a surrogate parameter for pulmonary tumor mass, was determined. ***P < .001 vs the vehicle control. **C**) Histological examination of representative sections from the indicated groups. **D**) Proliferation of tumor cells from mice treated with KINK-1 (3 mg/kg), doxorubicin (1 mg/kg), or KINK-1 and doxorubicin (3 mg/kg and 1 mg/kg, respectively). The PI (number of proliferating cells per 100 tumor cells) in acridine orange–stained lung sections was calculated based on at least 2000 tumor cells in each section, counted in a blinded fashion. Values represent the mean (with 95% confidence intervals [CIs]); ***P < .001; n.s. = not statistically significant (from two-sided t test). **E**) Treatment effects on established metastases. Lungs from C57BL6 mice injected intravenously with melanoma cells and left untreated for 8 days to allow tumor growth and then treated as indicated for another 12 days were weighed. Values represent the means (with 95% CIs, **P = .002 compared with vehicle control, ***P < .001 compared with both vehicle control and doxorubicin treatment by two-sided t test).

NF-κB (29,39–44). KINK-1 is the lead compound in a novel class of small-molecule inhibitors of IKKβ (45). The effectiveness of KINK-1 in inhibiting IKKβ activity was underscored by our observation of abrogation of constitutive and TNF-induced IκB phosphorylation in melanoma cells. Indeed, based on our observation that the compound suppressed constitutive NF-κB activation and

NF-κB activation induced by cytostatics or inflammatory agents, KINK-1 appears to be a universal inhibitor of NF-κB activation in melanoma cells, regardless of the mode of activation, which may vary considerably according to the inducer (41,46).

The distinct mechanisms of drug-induced activation of NF-κB were the basis for our selection of cytostatic agents in this study. Doxorubicin intercalates into DNA, where it forms adducts and inhibits topoisomerase II. This results in cell death (41,47). DNA-dependent protein kinase and the ataxia telangiectasia–mutated protein have been implicated in the activation of NF-κB following exposure to camptothecin (48,49). PMA is thought to activate NF-κB through stimulation of protein kinase C (PKC) α (50). Tamoxifen, an antiestrogen and PKC inhibitor, does not induce NF-κB activation but rather leads to a moderate attenuation of NF-κB signals in some cells (41). This suggests that the potentiation of tamoxifen's antiproliferative effect by KINK-1 results from additional NF-κB inhibition. In any case, specific inhibition of IKKβ, possibly augmented by weak inhibition of IKKα (51), appears to be a common denominator in KINK-1's inhibition of these various mechanisms for NF-κB activation.

Analysis of microarray data revealed that KINK-1 did not substantially affect expression of some gene products known to be important for the activity of cytostatics. These genes include DNA topoisomerases or proteins involved in the mitotic chromosome segregation machinery. Therefore, it appears that KINK-1 does not interfere directly with known mechanisms of cytostatic action but rather influences pathways that indirectly modulate the activity of cytostatic agents. One possible explanation for the increased effect of cytostatics in KINK-1–treated tumor cells may be provided by our observation of KINK-1–induced temporary G2 arrest of melanoma cells, which may facilitate DNA intercalation by cytostatic agents such as doxorubicin.

KINK-1 inhibition of IKKβ also led to marked decrease in expression of NF-κB–dependent gene products involved in cell proliferation, antiapoptosis, and invasion. Among them, both CXCL-8 (IL-8) and CCL-2 (MCP-1) have been implicated in angiogenesis, invasion, autocrine growth loops, and resistance to apoptosis; ICAM-1 and MMP-9 are essential for tumor cell invasion; TNFα, IL-6, CXCL-8, and IL-1α are mediators of immune responses; IL-1α, CXCL-2, CCL-2, and CCL-20 are involved in cell migration; and CXCL-1, CXCL-8, and COX-2 are associated with tumor growth, metastasis, and angiogenesis, respectively (52–59).

Although inhibition of NF-κB may in some cases induce cellular apoptosis (60–62), treatment with KINK-1 at concentrations that were therapeutic in mice did not by itself produce appreciable apoptosis in melanoma cells. However, given that exposure of melanoma cells to KINK-1 resulted in activation of some apoptotic responses such as release of mitochondrial cytochrome c and Smac, and a moderate decrease of some IAP proteins, it is reasonable to assume that increased apoptotic responses contribute to KINK-1's augmentation of antitumoral effects. Furthermore, at very high (approximately 25 μM) concentration, KINK-1 induced transient G2 arrest of the cell cycle or slowed G2/M progression in melanoma cells. Therefore, it is conceivable that KINK-1 at lower concentrations enhances the G2/M cell cycle arrest and subsequent apoptosis induced by cytostatic agents such as doxorubicin (63), camptothecin (64), or tamoxifen (65). Consistent with the idea that KINK-1 acts by targeting NF-κB, gene products under NF-κB control that are primarily or also regulated by other transcription factors, such as vascular endothelial growth factor and β-catenin, which depend on STAT-3 (66,67), were only marginally affected by KINK-1.

Overall, KINK-1 exhibited little toxicity at concentrations that were therapeutic in mice and sufficient for inhibition of IKKβ and potentiation of the antitumoral activity of several cytostatics. Toxicity of chemotherapeutics (eg, cardiotoxicity and neurotoxicity of anthracycline drugs) (68,69), is a major obstacle to achieving effective doses in humans. Therefore, enhancement of the antitumoral activity of doxorubicin at lower, less toxic doses would be very useful for cancer therapy. In mice, combined treatment with KINK-1 and doxorubicin led to a statistically significant decrease in experimental melanoma metastasis compared with either treatment alone. Higher doses of doxorubicin to achieve an equivalent effect would entail severe systemic toxicity.

In a model of pulmonary metastasis (70), we observed statistically significantly less tumor cell proliferation in situ in mice treated with a combination of doxorubicin and KINK-1 than in mice treated with either drug alone or vehicle. These mice also exhibited markedly fewer metastases within the lungs, consistent with our in vitro proliferation results. The marked reduction in the expression of proteins involved in cell proliferation in cells exposed to KINK-1 is likely to contribute to reduced tumor cell proliferation in vivo. However, the extent to which other systemic effects of NF-κB inhibition that were demonstrated in vitro, such as promotion of epithelial cell growth (71,72), immunosuppression (73), or IL-1β regulation (74), occur in vivo is difficult to predict.

Treatment of tumors with suboptimal doses of cytostatic agents may in some cases select for resistant cell clones, thus rendering the tumors even more recalcitrant to therapy. For example, doxorubicin, when used transiently at sublethal concentrations, renders tumor cells resistant to subsequent challenges (43,75). Enhancing the susceptibility of tumors to cytostatic agents using another compound, such as KINK-1, may provide a means to overcome chemoresistance in some cases. Melanoma cells isolated from lung metastases of mice treated with different concentrations of KINK-1 in vivo did not show altered responses to antitumoral treatment after they had been reestablished in vitro. Furthermore, because KINK-1 treatment did not lead to growth impairment (an indicator of long-term systemic toxicity) in mice when administered over a period of several weeks (45), it appears to be a safe treatment.

Our study has some limitations. First, it is unclear whether the antitumoral effect of KINK-1 will be observed following oral administration, the preferred route of administration for a small-molecule compound. Second, additional in vivo dose–response and toxicity experiments are needed to determine the optimal therapeutic window. Third, when used at therapeutic concentrations KINK-1 did not by itself induce appreciable apoptosis in melanoma cells. This finding, which is surprising in light of studies showing that inhibition of NF-κB may in some cases induce cellular apoptosis (61,62), suggests that IKKβ-dependent activation of NF-κB may not be sufficient for survival and tumorigenicity of cancer cells, a hypothesis that needs to be studied further. Fourth, our study did not explain why KINK-1 increased the antitumoral activity of some (eg, doxorubicin and camptothecin) but not all

cytostatics, and this question needs further study. Finally, it is necessary to investigate the efficacy of KINK-1 in additional preclinical tumor models, including melanoma models, addressing effects on local progression as well as other metastatic tumors.

In conclusion, our work suggests that using agents to enhance the susceptibility of tumor cells to cytostatic agents may improve future antitumoral regimens.

References

1. Grossman D, Altieri DC. Drug resistance in melanoma: mechanisms, apoptosis, and new potential therapeutic targets. *Cancer Metastasis Rev.* 2001;20(1–2):3–11.
2. Koon HB, Atkins MB. Update on therapy for melanoma: opportunities for patient selection and overcoming tumor resistance. *Expert Rev Anticancer Ther.* 2007;7(1):79–88.
3. Ollila DW. Complete metastasectomy in patients with stage IV metastatic melanoma. *Lancet Oncol.* 2006;7(11):919–924.
4. Serrone L, Zeuli M, Sega FM, Cognetti F. Dacarbazine-based chemotherapy for metastatic melanoma: thirty-year experience overview. *J Exp Clin Cancer Res.* 2000;19(1):21–34.
5. Lens MB, Eisen TG. Systemic chemotherapy in the treatment of malignant melanoma. *Expert Opin Pharmacother.* 2003;4(12):2205–2211.
6. Boon T, Coulie PG, van den Eynde BJ, van der Bruggen P. Human T cell responses against melanoma. *Annu Rev Immunol.* 2006;24:175–208.
7. Gajewski TF, Meng Y, Harlin H. Immune suppression in the tumor microenvironment. *J Immunother.* 2006;29(3):233–240.
8. Kirkwood JM, Moschos S, Wang W. Strategies for the development of more effective adjuvant therapy of melanoma: current and future exploration of antibodies, cytokines, vaccines, and combinations. *Clin Cancer Res.* 2006;12(7 pt 2):2331s–2336s.
9. Sinkovics JG, Horvath JC. Evidence accumulating in support of cancer vaccines combined with chemotherapy: a pragmatic review of past and present efforts. *Int J Oncol.* 2006;29(4):765–777.
10. Soengas MS, Lowe SW. Apoptosis and melanoma chemoresistance. *Oncogene.* 2003;22(20):3138–3151.
11. Ueda Y, Richmond A. NF-kappaB activation in melanoma. *Pigment Cell Res.* 2006;19(2):112–124.
12. Amiri KI, Richmond A. Role of nuclear factor-kappa B in melanoma. *Cancer Metastasis Rev.* 2005;24(2):301–313.
13. Ivanov VN, Bhoumik A, Ronai Z. Death receptors and melanoma resistance to apoptosis. *Oncogene.* 2003;22(20):3152–3161.
14. Nyormoi O, Bar-Eli M. Transcriptional regulation of metastasis-related genes in human melanoma. *Clin Exp Metastasis.* 2003;20(3):251–263.
15. Karin M, Lin A. NF-kappaB at the crossroads of life and death. *Nat Immunol.* 2002;3(3):221–227.
16. Kumar A, Takada Y, Boriek AM, Aggarwal BB. Nuclear factor-κB: its role in health and disease. *J Mol Med.* 2004;82(7):434–448.
17. Perkins ND. Integrating cell-signalling pathways with NF-κB and IKK function. *Nat Rev Mol Cell Biol.* 2007;8(1):49–62.
18. Karin M, Cao Y, Greten FR, Li ZW. NF-kappaB in cancer: from innocent bystander to major culprit. *Nat Rev Cancer.* 2002;2(4):301–310.
19. Karin M. Nuclear factor-κB in cancer development and progression. *Nature.* 2006;441(7092):431–436.
20. Shishodia S, Aggarwal BB. Nuclear factor-κB activation: a question of life and death. *J Biochem Mol Biol.* 2002;35(1):28–40.
21. Karin M, Yamamoto Y, Wang QM. The IKK NF-κB system: T treasure trove for drug development. *Nat Rev Drug Discov.* 2004;3(1):17–26.
22. Scheidereit C. IκB kinase complexes: gateways to NF-κB activation. *Oncogene.* 2006;25(51):6685–6705.
23. Das KC, White CW. Activation of NF-kappaB by antineoplastic agents. Role of protein kinase C. *J Biol Chem.* 1997;272(23):14914–14920.
24. Pikarsky E, Porat RM, Stein I, et al. NF-κB functions as a tumor promotor in inflammation-associated cancer. *Nature.* 2004;431(7007):461–466.
25. Greten FR, Eckmann L, Greten TF, et al. IKKβ links inflammation and tumorigenesis in a mouse model of colitis-associated cancer. *Cell.* 2004;118(6):285–296.
26. Luo JL, Maeda S, Hsu LC, Yagita H, Karin M. Inhibition of NF-κB in cancer cells converts inflammation-induced tumor growth mediated by TNFα to TRAIL-mediated tumor regression. *Cancer Cell.* 2004;6(3):297–305.
27. Huber W, von Heydebreck A, Sultmann H, Poustka A, Vingron M. Variance stabilization applied to microarray data calibration and to the quantification of differential expression. *Bioinformatics.* 2002;18(suppl 1):s96–s104.
28. Murata T, Shimada M, Sakakibara S, et al. Synthesis and structure-activity relationships of novel IKK-β inhibitors. Part 3: orally active anti-inflammatory agents. *Bioorg Med Chem Lett.* 2004;14(15):4019–4022.
29. Kunnumakkara AB, Guha S, Krishnan S, Diagaradjane P, Gelovani J, Aggarwal BB. Curcumin potentiates antitumor activity of gemcitabine in an orthotopic model of pancreatic cancer through suppression of proliferation, angiogenesis, and inhibition of nuclear factor-κB-regulated gene products. *Cancer Res.* 2007;67(18):3853–3861.
30. Schön M, Bong AB, Drewniok C, et al. Tumor-selective induction of apoptosis and the small-molecule immune response modifier imiquimod. *J Natl Cancer Inst.* 2003;95(15):1138–1149.
31. Schön MP, Wienrich BG, Drewniok C, et al. Death receptor-independent apoptosis in malignant melanoma induced by the small-molecule immune response modifier imiquimod. *J Invest Dermatol.* 2004;122(5):1266–1276.
32. Oostingh GJ, Schlickum S, Friedl P, Schön MP. Impaired induction of adhesion molecule expression in immortalized endothelial cells leads to functional defects in dynamic interactions with lymphocytes. *J Invest Dermatol.* 2007;127(9):2253–2258.
33. McGahon AJ, Martin SJ, Bissonnette RP, et al. The end of the (cell) line: methods for the study of apoptosis in vitro. *Methods Cell Biol.* 1995;46:153–185.
34. Ghosh S, Karin M. Missing pieces in the NF-kappaB puzzle. *Cell.* 2002;109(suppl 1):S81–S96.
35. Manna S, Mukhopadhyay A, Aggarwal BB. Resveratrol suppresses TNF-induced activation of nuclear transcription factors NF-κB, activator protein-1, and apoptosis: potential role of reactive oxygen intermediates and lipid peroxidation. *J Immunol.* 2000;164(12):6509–6519.
36. Baldini N. Multidrug resistance—a multiplex phenomenon. *Nat Med.* 1997;3(4):378–380.
37. Abe S, Hasegawa M, Yamamoto K, et al. Rapid induction of IAP family proteins and Smac/DIABLO expression after proapoptotic stimulation with doxorubicin in RPMI 8226 multiple myeloma cells. *Exp Mol Pathol.* 2007;83(3):405–412.
38. Wang CY, Guttridge DC, Mayo MW, Baldwin AS Jr. NF-kappaB induces expression of the Bcl-2 homologue A1/Bfl-1 to preferentially suppress chemotherapy-induced apoptosis. *Mol Cell Biol.* 1999;19(9):5923–5929.
39. Liem AA, Chamberlain MP, Wolf CR, Thompson AM. The role of signal transduction in cancer treatment and drug resistance. *Eur J Surg Oncol.* 2002;28(6):679–684.
40. Bian X, McAllister-Lucas LM, Shao F, Schumacher KR, Feng Z, Porter AG, Castle VP, Opipari AW Jr. NF-kappa B activation mediates doxorubicin-induced cell death in N-type neuroblastoma cells. *J Biol Chem.* 2001;276(52):48921–48929.
41. Chuang SE, Yeh PY, Lu YS, et al. Basal levels and patterns of anticancer drug-induced activation of nuclear factor-kappaB (NF-kappaB), and its attenuation by tamoxifen, dexamethasone, and curcumin in carcinoma cells. *Biochem Pharmacol.* 2002;63(9):1709–1716.
42. Li Y, Ahmed F, Ali S, Philip PA, Kucuk O, Sarkar FH. Inactivation of nuclear factor kappaB by soy isoflavone genistein contributes to increased apoptosis induced by chemotherapeutic agents in human cancer cells. *Cancer Res.* 2005;65(15):6934–6942.
43. Yeh PY, Chuang SE, Yeh KH, Song YC, Ea CK, Cheng AL. Increase of the resistance of human cervical carcinoma cells to cisplatin by inhibition of the MEK to ERK signaling pathway partly via enhancement of anticancer drug-induced NF kappa B activation. *Biochem Pharmacol.* 2002;63(8):1423–1430.
44. Luo JL, Kamata H, Karin M. IKK/NF-kappaB signaling: balancing life and death—a new approach to cancer therapy. *J Clin Invest.* 2005;115(10):2625–2632.
45. Ziegelbauer K, Gantner F, Lukacs NW, et al. A selective novel low-molecular-weight inhibitor of IkappaB kinase-beta (IKK-beta) prevents

pulmonary inflammation and shows broad anti-inflammatory activity. *Br J Pharmacol.* 2005;145(2):178–192.
46. Pahl HL. Activators and target genes of Rel/NF-κB transcription factors. *Oncogene.* 1999;18(49):6853–6866.
47. Gewirtz DA. A critical evaluation of the mechanisms of action proposed for the antitumor effects of the anthracycline antibiotics adriamycin and daunorubicin. *Biochem Pharmacol.* 1999;57(7):727–741.
48. Basu S, Rosenzweig KR, Youmell M, Price BD. The DNA-dependent protein kinase participates in the activation of NF kappa B following DNA damage. *Biochem Biophys Res Commun.* 1998;247(1):79–83.
49. Piret B, Schoonbroodt S, Piette J. The ATM protein is required for sustained activation of NF-kappaB following DNA damage. *Oncogene.* 1999;18(13):2261–2271.
50. Shin Y, Yoon SH, Choe SH, et al. PMA-induced up-regulation of MMP-9 is regulated by a PKCα-NF-κB cascade in human lung epithelial cells. *Exp Mol Med.* 2007;39(1):97–105.
51. O'Mahoney A, Lin X, Geleziunas R, Greene WC. Activation of the heterodimeric IkappaB kinase alpha (IKKalpha)-IKKbeta complex is directional: IKKalpha regulates IKKbeta under both basal and stimulated conditions. *Mol Cell Biol.* 2000;20(4):1170–1178.
52. Aoudjit F, Potworowski EF, Springer TA, St-Pierre Y. Protection from lymphoma cell metastasis in ICAM-1 mutant mice: a posthoming event. *J Immunol.* 1998;161(5):2333–2338.
53. Homey B, Müller A, Zlotnik A. Chemokines: agents for the immunotherapy of cancer?. *Nat Rev Immunol.* 2002;2(3):175–184.
54. Dhawan P, Richmond A. Role of CXCL1 in tumorigenesis of melanoma. *J Leukoc Biol.* 2002;72(1):9–18.
55. Payne AS, Cornelius LA. The role of chemokines in melanoma tumor growth and metastasis. *J Invest Dermatol.* 2002;118(6):915–922.
56. van Damme J, Struyf S, Opdenakker G. Chemokine-protease interactions in cancer. *Semin Cancer Biol.* 2004;14(3):201–208.
57. Altinoz MA, Korkmaz R. NF-kappaB, macrophage migration inhibitory factor and cyclooxygenase-inhibitions as likely mechanisms behind the acetaminophen- and NSAID-prevention of the ovarian cancer. *Neoplasma.* 2004;51(4):239–247.
58. Liao Z, Mason KA, Milas L. Cyclo-oxygenase-2 and its inhibition in cancer: is there a role? *Drugs.* 2007;67(6):821–845.
59. Bertagnolli MM. Chemoprevention of colorectal cancer with cyclooxygenase-2 inhibitors: two steps forward, one step back. *Lancet Oncol.* 2007; 8(5):439–443.
60. Notarbartolo M, Cervello M, Poma P, Dusonchet L, Meli M, DÁlessandro N. Expression of the IAPs in multidrug resistant tumor cells. *Oncol Rep.* 2004;11(1):133–136.
61. Bush JH, Cheung KJJ, Li G. Curcumin induces apoptosis in human melanoma cells through a Fas receptor/caspase-8 pathway independent of p53. *Exp Cell Res.* 2001;271(2):301–314.
62. Woo JH, Kim YH, Choi YJ, et al. Molecular mechanisms of curcumin-induced cytotoxicity: induction of apoptosis through generation of reactive oxygen species, down-regulation of Bcl-XL and IAP, the release of cytochrome c and inhibition of Akt. *Carcinogenesis.* 2003;24(7): 1199–1208.
63. Dubrez L, Goldwasser F, Genne P, Pommier Y, Solary E. The role of cell cycle regulation and apoptosis triggering in determining the sensitivity of leukemic cells to topoisomerase I and II inhibitors. *Leukemia.* 1995;9(6): 1013–1024.
64. Goldwasser F, Shimizu T, Jackman J, et al. Correlations between S and G2 arrest and the cytotoxicity of camptothecin in human colon carcinoma cells. *Cancer Res.* 1996;56(19):4430–4437.
65. Sutter AP, Maaser K, Grabowski P, et al. Peripheral benzodiazepine receptor ligands induce apoptosis and cell cycle arrest in human hepatocellular carcinoma cells and enhance chemosensitivity to paclitaxel, docetaxel, doxorubicin and the Bcl-2 inhibitor HA14-1. *J Hepatol.* 2004;41(5):799–807.
66. Kawada M, Seno H, Uenoyama Y, et al. Signal transducers and activators of transcription 3 activation is involved in nuclear accumulation of beta-catenin in colorectal cancer. *Cancer Res.* 2006;66(6):2913–2917.
67. Chen Z, Han ZC. STAT3: a critical transcription activator in angiogenesis. *Med Res Rev.* 2008;28(2):185–200.
68. Jones RL, Swanton C, Ewer MS. Anthracycline cardiotoxicity. *Expert Opin Drug Saf.* 2006;5:(6)791–809.
69. Barry E, Alvarez JA, Scully RE, Miller TL, Lipshultz SE. Anthracycline-induced cardiotoxicity: course, pathophysiology, prevention and management. *Expert Opin Pharmacother.* 2007;8(8):1039–1058.
70. Mockey M, Bourseau E, Chandrashekhar V, et al. mRNA-based cancer vaccine: prevention of B16 melanoma progression and metastasis by systemic injection of MART1 mRNA histidylated lipopolyplexes. *Cancer Gene Ther.* 2007;14(9):802–814.
71. Seitz CS, Deng H, Hinata K, Lin Q, Khavari PA. Nuclear factor-kappa B subunits induce epithelial cell growth arrest. *Cancer Res.* 2000;60(15): 4085–4092.
72. van Hogerlinden M, Rozell BL, Toftgard R, Sundberg JP. Characterization of the progressive skin disease and inflammatory cell infiltrate in mice with inhibited NF-κB signaling. *J Invest Dermatol.* 2004;123(1):101–108.
73. Liang Y, Zhou Y, Shen P. NF-kappaB and its regulation on the immune system. *Cell Mol Immunol.* 2004;1(5):343–350.
74. Greten FR, Arkan MC, Bollrath J, et al. NF-kappaB is a negative regulator of IL-1 beta secretion as revealed by genetic and pharmacological inhibition of IKKbeta. *Cell.* 2007;130(5):918–931.
75. Yeh PY, Chuang SE, Yeh KH, Song YC, Cheng AL. Involvement of nuclear transcription factor-kappa B in low-dose doxorubicin-induced drug resistance of cervical carcinoma cells. *Biochem Pharmacol.* 2003;66(1):25–33.

Funding

Deutsche Forschungsgemeinschaft (Rudolf Virchow Award to M.P.S.); Deutsche Krebshilfe/Dr. Mildred Scheel-Stiftung (10-2196 Schö-2); Interdisciplinary Collaborative Clinical Research Center (project B-20-N to M.S. and M.P.S.).

Notes

The authors take full responsibility for the study design, data collection, analysis and interpretation of the data, the decision to submit the manuscript for publication, and the writing of the manuscript.

Manuscript received November 6, 2007; revised April 30, 2008; accepted May 2, 2008.